

# Stability Region of Fractional-Order PI Controller for a Single-Area Load Frequency Control System with Communication Time Delay

**Şahin Sönmez**

Department of Electrical and Electronics Engineering, Niğde Ömer Halisdemir University, Main Campus, 51240 Nigde, Turkey  
sahinsonmez@ohu.edu.tr

**Saffet Ayasun**

Department of Electrical and Electronics Engineering, Niğde Ömer Halisdemir University, Main Campus, 51240 Nigde, Turkey  
sayasun@ohu.edu.tr

**Abstract**—In this paper, an effective graphical method is utilized to compute the stabilizing values of Fractional Order Proportional Integral (FOPI) controller parameters of a single-area Load Frequency Control (LFC) system with communication time delay. The approach is based on the stability boundary locus, which can be easily obtained by equating the real and the imaginary parts of the characteristic equation to zero. The stability regions are displayed in FOPI controller parameters space. Finally, time-domain simulation studies are carried to prove the accuracy and effectiveness of the proposed method.

**Keywords**— Fractional order PI control, Load frequency control, Stability region, Stabilization, Time delays

## I. INTRODUCTION

Time delays are observed in load frequency control (LFC) systems due to extensive use of phasor measurement units (PMUs) and communication links used to transmit data from power plant to central controller [1, 2]. The main goals of LFC systems are to control the frequency and to maintain scheduled power interchange in an interconnected system with one or more independently controlled areas. For that purpose, in LFC systems, conventional (integer order) proportional-integral (PI) and proportional-integral-derivative (PID) controllers are generally adopted to improve the dynamic frequency response and to eliminate or reduce the steady-state errors in frequency [3]. Recently, fractional order PI and PID controllers are proposed for LFC systems [4, 5]. It has been reported that fractional order controllers ensures good stability and dynamic performance of LFC systems. For example, fractional order controllers result in less rise time, overshoots and settling time than conventional integer order controllers [4]. However, in these recent studies, time delays due to communication links were ignored in FOPI controller design of LFC systems. Large amount of communication delays in the range of 5-15 s are generally observed in LFC systems [6-8]. Therefore,

such delays should not be ignored and must be taken into account in the design of classical PI and/or FOPI controller design.

The existing studies in the stability analysis of time-delayed LFC systems mainly focus on conventional controller design and the stability delay margin computation for a given set of controller parameters. In [6], a control design method based on linear matrix inequalities (LMIs) is suggested for LFC systems with communication delays. In [9, 10], robust decentralized PI control design methods based on  $H_2/H_\infty$  control technique and a real-time implementation are proposed for LFC with communication delays. The work reported in [11] deals with the designing of delay-dependent two-term  $H_\infty$  controller for stabilizing and load disturbance rejection for a two-area LFC model with multiple state delays. Delay margin computation methods could be grouped into two main types, namely frequency-domain direct and time-domain indirect methods. The main goal of frequency domain approaches is to compute all critical purely imaginary roots of the characteristic equation for which the system will be marginally stable. The following three methods are the ones commonly used in delay margin computation of power systems: i) Schur-Cohn method [12]; ii) Elimination of exponential terms in the characteristic equation [13]; iii) Rekasius substitution [14, 15]. Among these direct methods, the Schur-Chon approach has been successfully implemented to compute the delay margin for automatic generation control (AGC) systems [8]. The Rekasius substitution has been efficiently used to determine delay margins for a single-area LFC system with conventional PI controller [16]. The indirect time-domain methods that utilize Lyapunov stability theory and linear matrix inequalities (LMIs) techniques have been used to estimate delay margins of the LFC systems with conventional PI controller [7, 17].

For a complete picture of LFC system stability, it is essential to determine all possible values of conventional PI and/or FOPI control parameters that ensure a stable operation when certain amount of time delays are observed.

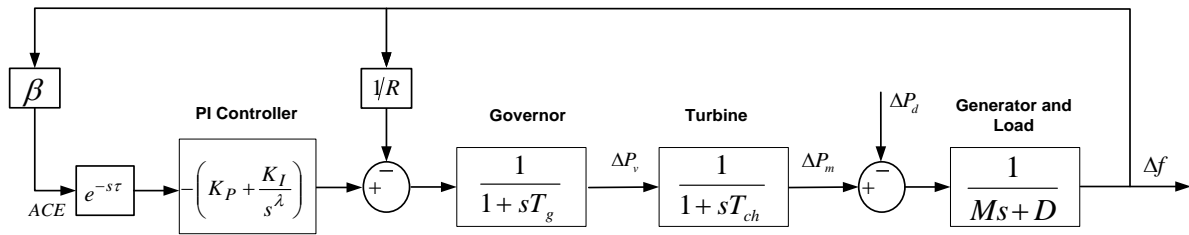


Fig.1. Block diagram of a single area LFC system with a communication delay and FOPI controller

This paper utilizes a graphical method to compute the stabilizing values of FOPI controller parameters over a possible smaller range of frequency. The approach is based on the stability boundary locus, which can be easily obtained by equating the real and the imaginary parts of the characteristic equation to zero [18, 19]. The proposed method has been effectively applied to controller design and synthesis of LFC system without time delays, time-delayed integrating systems and large wind turbine systems [5, 20, 21].

In this paper, the stability regions for single-area time-delayed LFC system are displayed in FOPI controller parameters space,  $(K_I, K_P)$  plane. The complete stabilizing set in this plane can be identified immediately based on the presented method, rather than computed mathematically. The impacts of the time delay and the fractional order of the integrator on the stability region of PI controller gains are analyzed. It has been observed that the stability region becomes smaller as the time delay increases and the FOPI controller gives a larger stability region than the conventional PI controller when the fractional order of the integrator is greater than one. With the help of time-domain simulations, the accuracy and effectiveness of the proposed method are also verified.

## II. COMPUTATION OF STABILITY REGION IN FOPI CONTROLLER PARAMETER SPACE

The block diagram of a single-area LFC system is shown in Fig. 1. The conventional LFC model is modified to take into account the communication time delay into the control loop. The generator is assumed to be equipped with a non-reheat turbine. A FOPI controller is included in the model. For stability analysis, it is necessary to obtain the characteristic equation of time-delayed LFC system given as follows:

$$\Delta(s, \tau) = P(s) + Q(s)e^{-s\tau} = 0 \quad (1)$$

$$P(s) = p_3s^3 + p_2s^2 + p_1s + p_0; \quad Q(s) = \beta R \left( K_P + \frac{K_I}{s^\lambda} \right)$$

$$p_3 = MRT_g T_{ch}, \quad p_2 = MRT_{ch} + RDT_g T_{ch} + MRT_g, \\ p_1 = MR + RDT_{ch} + RDT_g, \quad p_0 = RD + 1$$

where  $\tau$  is the total time delay,  $P(s)$  and  $Q(s)$  are polynomials in  $s$  with real coefficients and  $\lambda$  is fractional order (FO) of the integrator in the PI controller.  $M, D, T_g, T_{ch}, R,$  and  $\beta$  denote the moment of inertia of the generator, generator damping coefficient, time constant of the governor, time constant of the turbine, speed drop, and frequency bias factor, respectively.

The aim of this paper is to determine the parameter set  $(K_I, K_P)$  of the FOPI controller for which the LFC system is stable. For that purpose, the

characteristic equation of the LFC system given in (1) is first rewritten as

$$\Delta(s, \tau, \lambda) = \beta R e^{-s\tau} (K_P s^\lambda + K_I) + p_3 s^{3+\lambda} + p_2 s^{2+\lambda} + p_1 s^{1+\lambda} + p_0 s^\lambda = 0 \quad (2)$$

Then, in order to obtain the boundary of the stabilizing region, we substitute  $s = j\omega$  and  $\omega > 0$  into (2) as follows:

$$\Delta(j\omega, \tau, \lambda) = \beta R e^{-j\omega\tau} (K_P (j\omega)^\lambda + K_I) + p_3 (j\omega)^{3+\lambda} + p_2 (j\omega)^{2+\lambda} + p_1 (j\omega)^{1+\lambda} + p_0 (j\omega)^\lambda = 0 \quad (3)$$

Substituting  $e^{-j\omega\tau} = \cos(\omega\tau) - j\sin(\omega\tau)$  into (3) we obtain the following characteristic equation.

$$\Delta(j\omega, \tau, \lambda) = \beta R (\cos \omega\tau - j \sin \omega\tau) (K_P (e + jf) + K_I) + \sum_{i=0}^3 p_i (c_i + j d_i) = 0 \\ \Delta(j\omega, \tau, \lambda) = [K_P (\beta R e \cos \omega\tau + \beta R f \sin \omega\tau) + K_I (\beta R \cos \omega\tau) + \sum_{i=0}^3 p_i c_i] + j [K_P (\beta R f \cos \omega\tau - \beta R e \sin \omega\tau) + K_I (-\beta R \sin \omega\tau) + \sum_{i=0}^3 p_i d_i] \\ = \Re \{ \Delta(j\omega, \tau, \lambda) \} + j \Im \{ \Delta(j\omega, \tau, \lambda) \} = 0 \quad (4)$$

where  $\Re\{\Delta(j\omega, \tau, \lambda)\}$  and  $\Im m\{\Delta(j\omega, \tau, \lambda)\}$  represent the real and imaginary parts of the characteristic equation, respectively, and

$$e = \Re\{(j\omega)^\lambda\}, \quad f = \Im m\{(j\omega)^\lambda\},$$

$$c_i = \Re\{(j\omega)^{i+\lambda}\}, \quad d_i = \Im m\{(j\omega)^{i+\lambda}\}$$

The noninteger power of a complex number  $(j\omega)^\lambda$  can be easily computed using any scientific software packages. Then, equating the real and imaginary parts of (4) to zero, one obtains

$$\begin{aligned} K_P A(\omega) + K_I B(\omega) + C(\omega) &= 0 \\ K_P D(\omega) + K_I E(\omega) + F(\omega) &= 0 \end{aligned} \quad (5)$$

where

$$\begin{aligned} A(\omega) &= \beta R e \cos \omega \tau + \beta R f \sin \omega \tau; \quad B(\omega) = \beta R \cos \omega \tau \\ C(\omega) &= \sum_{i=0}^3 p_i c_i; \quad D(\omega) = \beta R f \cos \omega \tau - \beta R e \sin \omega \tau \\ E(\omega) &= -\beta R \sin \omega \tau; \quad F(\omega) = \sum_{i=0}^3 p_i d_i \end{aligned} \quad (6)$$

Solving (5) for  $K_P$  and  $K_I$  we obtain

$$\begin{aligned} K_P &= \frac{B(\omega)F(\omega) - E(\omega)C(\omega)}{A(\omega)E(\omega) - B(\omega)D(\omega)} \\ K_I &= \frac{D(\omega)C(\omega) - A(\omega)F(\omega)}{A(\omega)E(\omega) - B(\omega)D(\omega)} \end{aligned} \quad (7)$$

Solving these two equations in (7) simultaneously, the stability boundary locus  $\ell(K_P, K_I, \omega)$  in the  $(K_I, K_P)$  plane could be obtained. The stability boundary locus,  $\ell(K_P, K_I, \omega)$  and the line  $K_I = 0$ , divide the parameter plane,  $(K_I, K_P)$ -plane, into stable and unstable regions. Choosing a test point within each region, the stable region that contains the values of stabilizing  $K_P$  and  $K_I$  parameters can be determined. Note that the line  $K_I = 0$  is also in the boundary locus since a real root of  $\Delta(s, \tau) = 0$  can cross the imaginary axis at  $s = 0$ . From the imaginary parts of (4), it can be found that for  $\omega = 0$ ,  $\Im m\{\Delta(j\omega, \tau, \lambda)\} = 0$  and from  $\Re\{\Delta(j\omega, \tau, \lambda)\} = 0$ , the integral controller gain is obtained as  $K_I = 0$ . This part of the boundary locus is known as the Real Root Boundary (RRB) and the one obtained from (7) is defined as the Complex Root Boundary (CRB) of the stability region [18, 19].

### III. RESULTS

For a selected range of crossing frequencies  $\omega$  and delay value, the stability boundary locus and stability regions of the single-area LFC system for different values of FO of the integral ( $\lambda$ ) are obtained. The LFC system parameters used in this paper are as follows:  $T_{ch} = 0.3$  s,  $T_g = 0.1$  s,  $R = 0.05$ ,  $D = 1.0$ ,  $\beta = 21$ ,  $M = 10$  s.

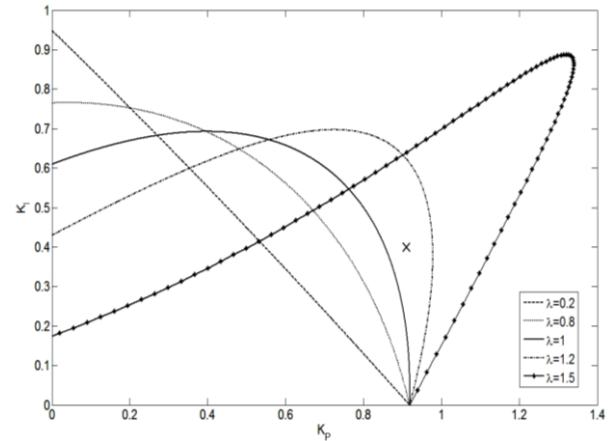


Fig. 2. Stability regions for various values of  $\lambda$  when  $\tau = 2$  s.

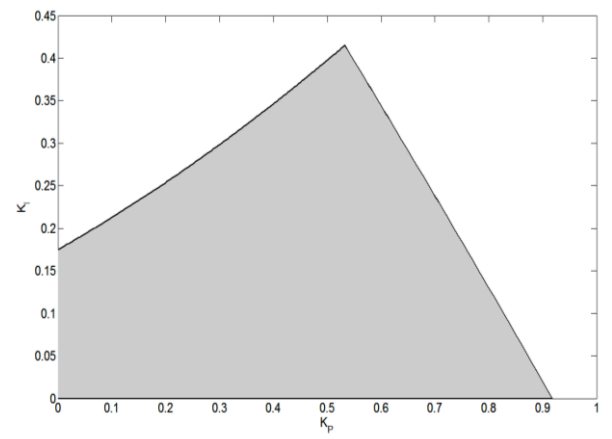


Fig. 3. Reliable stability region for FOPI controllers when  $\tau = 2$  s.

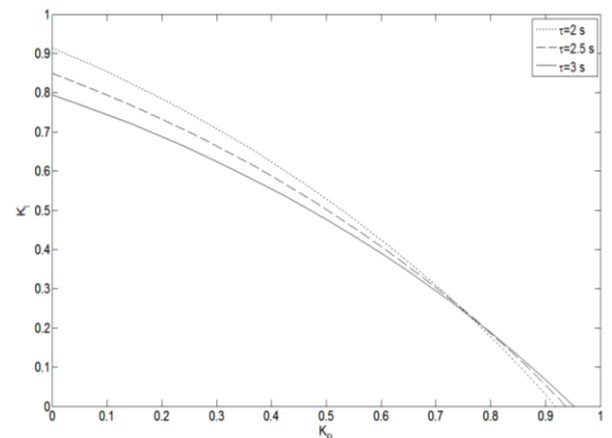


Fig. 4. The effect of time delay on the stability region for  $\lambda = 0.5$ .

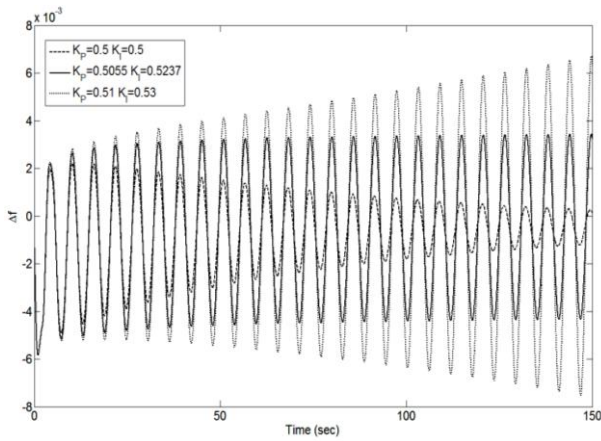


Fig. 5. Frequency deviation for three different values of  $(K_I, K_P)$  when  $\lambda = 0.5$  and  $\tau = 2$  s.

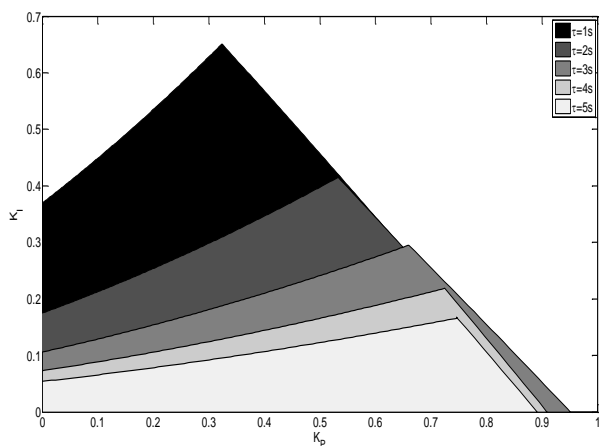


Fig. 6. Reliable stability region for different values of time delay.

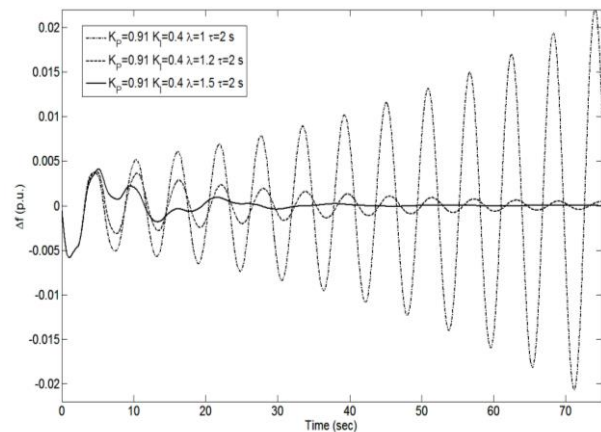


Fig. 7. Stabilizing effect of FOPI controller for  $\tau = 2$  s.

Fig. 2 shows stability regions for  $\lambda = 0.2$ ,  $\lambda = 0.8$ ,  $\lambda = 1.0$ ,  $\lambda = 1.2$ , and  $\lambda = 1.5$  when the delay is  $\tau = 2$  s. This figure clearly indicates that the fractional order of the integral ( $\lambda$ ) has a significant impact on both size and shape of the stability region. It is noted from this figure that both  $\lambda = 1.2$  and  $\lambda = 1.5$  result in a bigger stability region than integer value of  $\lambda = 1.0$ . The reliable stability region which is the intersection of these stability regions is shown Fig. 3. In order to

show the effect of time delay, we choose different values of time delay. Fig. 4 illustrates stability regions for  $\tau = 2$  s,  $\tau = 2.5$  s, and  $\tau = 3.0$  s when the fractional order of the integral is fixed at  $\lambda = 0.5$ . It can be seen that the stability region shrinks slightly for almost all values of  $K_P$  as time delay increases. Finally, Fig. 5 shows frequency deviations for three different values of  $(K_I, K_P)$  when  $\lambda = 0.5$  and  $\tau = 2$  s for a  $0.1$  pu step increase in the load  $\Delta P_d$  at  $t = 0$  s. The controller gains are  $K_I = 0.5, K_P = 0.5$  located inside the stability region shown in Fig. 4,  $K_I = 0.5055, K_P = 0.5237$  right on the stability boundary, and  $K_I = 0.51, K_P = 0.53$  located outside the stability region. Fig. 5 clearly indicates that the LFC system is marginally stable for  $K_I = 0.5055, K_P = 0.5237$  since sustained oscillations are observed in the frequency deviation. For  $K_I = 0.5, K_P = 0.5$ , the LFC system is stable since oscillations are decaying. Finally, for  $K_I = 0.51, K_P = 0.53$ , the LFC system becomes unstable due to the growing oscillations, indicating the oscillatory instability. The time-domain simulation results have confirmed the accuracy of the proposed method. Furthermore, the effect of the time delay on the reliable stability region is investigated. Fig. 6 shows how the reliable stability region changes with respect to the time delay laying in a range of  $\tau = 1 - 5$  s. Observe that the shape of the region does not change much. On the other hand, the reliable stability region gets smaller as the time delay increases.

Finally, the stabilizing effect of FOPI controller is illustrated in Fig. 7 for  $\tau = 2$  s. The controller parameters are chosen as  $K_I = 0.4, K_P = 0.91$ . As can be seen from Fig. 2, these parameter values displayed using a cross sign are located outside the stability region of conventional PI controller ( $\lambda = 1$ ) and inside the stability regions of FOPI controller for both  $\lambda = 1.2$  and  $\lambda = 1.5$ . Fig. 7 clearly shows that the LFC system becomes unstable due to growing oscillations in the frequency deviation when the conventional PI controller is used. However, the usage of FOPI controller for the same parameter values stabilizes the time-delayed LFC system as illustrated in Fig. 7 for both  $\lambda = 1.2$  and  $\lambda = 1.5$ .

#### IV. CONCLUSION AND FUTURE WORK

In this paper, a graphical method has been implemented to determine the boundaries of limiting values of both conventional PI and fractional order PI controller parameters that ensure the stability of single-area LFC system with communication time delay. The method is based on the stability boundary locus that is obtained by equating the real and the imaginary parts of the characteristic equation to zero. The effect of time delay and order of integral controller has been investigated. The results indicate that the stability region becomes smaller as the time delay increases. Moreover, the use of FOPI controller

results in a larger set of stabilizing controller parameters for time-delayed LFC systems. The time-domain simulations show that FOPI controller has a better stabilization performance than conventional PI controller for the time-delay LFC system. As future work, the effect of fractional order derivative control on the stabilization of LFC system with time delay will be investigated and the proposed method will be extended to multi-area LFC systems with communication delays.

#### REFERENCES

- [1] B. Naduvathuparambil, M.C. Valenti, and A. Feliachi, "Communication delays in wide area measurement systems," In: Proceedings of the 34th southeastern symposium on system theory, University of Alabama, Huntsville, pp. 118-122, March 2005.
- [2] X. Xia, Y. Xin, J. Xiao, J. Wu, and Y. Han, "WAMS Applications in Chinese power systems," IEEE Power and Energy Magazine, vol. 4, pp. 54-63, Jan.- Feb. 2006.
- [3] P. Kundur, Power system stability and control. McGraw-Hill Inc., New York, 1994.
- [4] M.I. Alomoush, "Load frequency control and automatic generation control using fractional-order controllers," Electrical Engineering, vol. 91, pp. 357-368, Jan. 2010.
- [5] S. Sondhi, and Y.V. Hote, "Fractional-order PID controller for load frequency control," Energy Conversion and Management, vol. 85, pp. 343-353, Sept. 2014.
- [6] X. Yu, and K. Tomsovic, "Application of linear matrix inequalities for load frequency control with communication delays," IEEE Trans on Power Syst., vol. 19, pp. 1508-1515, August 2004.
- [7] L. Jiang, W. Yao, Q.H. Wu, J.Y. Wen, and S.J. Cheng, "Delay-dependent stability for load frequency control with constant and time-varying delays," IEEE Trans Power Syst, vol. 27, pp. 932-941, May. 2012.
- [8] M. Liu, L. Yang, D. Gan, D. Wang, F. Gao, and Y. Chen, "The stability of AGC systems with commensurate delays," Euro Trans Electr Power, vol. 17, pp. 615-627, Nov. 2007.
- [9] H. Bevrani, and T. Hiyama, "Robust decentralized PI based LFC design for time delay power systems," Energy Conversion and Management, vol. 49, pp. 193-204, Feb. 2008.
- [10] H. Bevrani, and T. Hiyama, "On load-frequency regulation with time delays: Design and real-time implementation," IEEE Trans Energy Conversion, vol. 24, pp. 292-300, March 2009.
- [11] R. Day, S. Ghosh, and A. Rakshit, " $H^\infty$  Load frequency control of interconnected power systems with communication delays," Electrical Power and Energy Systems, vol. 42, pp. 672-684, 2012.
- [12] J. Chen, G. Gu, and C.N. Nett, "A new method for computing delay margins for stability of linear delay systems," System and Control Letters, vol. 26, pp. 107-117, Sept. 1995.
- [13] K.E. Walton, and J.E. Marshall, "Direct method for TDS stability analysis," IEE Proceeding Part D, vol. 134, pp. 101-107, 1987.
- [14] Z.V. Rekasius, "A stability test for systems with delays," The Joint Automatic Control Conference, , San Francisco, CA, Paper No. TP9-A, 1980.
- [15] N. Olgac, and R. Sipahi, "An exact method for the stability analysis of time-delayed linear time-invariant (LTI) systems," IEEE Trans Autom Control, vol. 47, pp. 793-797, May. 2002.
- [16] Ş. Sönmez, S. Ayasun, and U. Eminoğlu, "Computation of time delay margin for stability of a single-area load frequency control system with communication delays," WSEAS Trans Power Syst., vol. 9, pp. 67-76, 2014.
- [17] C.K. Zhang, L. Jiang, and Q. Wu, "Further results on delay-dependent stability of multi-area load frequency control," IEEE Trans Power Syst., vol. 28, pp. 4465-4474, Nov. 2013.
- [18] M.T. Söylemez, N. Munro, and H. Baki, "Fast calculation of stabilizing PID controller," Automatica, vol. 39, pp. 121-126, Jan. 2003.
- [19] N. Tan, I. Kaya, C. Yeroglu, and D.P. Atherton, "Computation of stabilizing PI and PID controllers using the stability boundary locus," Energy Conversion and Management, vol. 47, pp. 3045-3058, Nov. 2006.
- [20] S.E. Hamamcı, and M. Köksal, "Calculation of all stabilizing fractional-order PD controllers for integrating time delay systems," Computers and Mathematics with Applications, vol. 59, pp. 1621-1629, 2010.
- [21] J. Wang, N. Tse, and Z. Gao, "Synthesis on-PI-based pitch controller of large wind turbine generator," Energy Conversion and Management, vol. 52, pp. 1288-1294, Feb. 2011.